Supplement of Atmos. Meas. Tech., 13, 6853–6875, 2020
https://doi.org/10.5194/amt-13-6853-2020-supplement

Atmospheric Measurement Techniques
Open Access
EGU

Supplement of

Absolute calibration method for frequency-modulated continuous wave (FMCW) cloud radars based on corner reflectors

Felipe Toledo et al.

Correspondence to: Felipe Toledo (ftoledo@lmd.polytechnique.fr)

S1 The Radar Equation

This section describes how to derive the absolute reflectivity calibration terms of a Frecuency Modulated Continuous Wave (FMCW) radar. This procedure can also be applied for pulsed doppler radars by using their corresponding radar equation.

The radar equation describes the physical power budget of a signal emitted by the radar from the instant it enters the transmitter antenna until it is received by the receiver antenna. At the beginning, the transmitted signal is generated by the radar emitter chain. This signal enters the emitter antenna with a power P'_t (physical power, for example in watt units). Usually radar antennas are very directive, with its main lobe oriented in the direction of observation. The maximum gain of the main transmitter antenna lobe is defined as G_t.

Figure S1 shows the geometrical configuration of a system with a radar and an scattering object placed at a distance r. Assuming the radar transmitter antenna is aligned in the angle of maximum gain with this target, the object will receive a power density P_{rec} of:

$$P_{rec} = P'_t \frac{G_t}{4\pi r^2} \tag{S1}$$

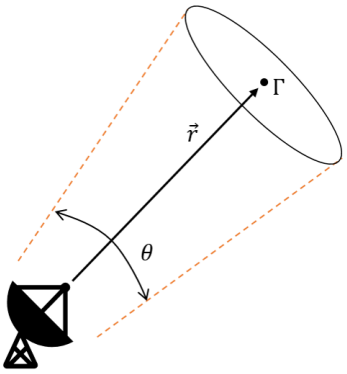

Figure S1: Radar pointing towards a target with cross section Γ, located at a distance r. θ is the beam width of the antennas.

The Radar Cross Section (RCS) Γ of an object can be understood as the equivalent cross-sectional area a sphere should have to reflect the same amount of incident power back to the radar receiver. The units to represent RCS are m^2 in physical scale, and $dBsm$ in dB scale ($dBsm = 10\log_{10}(\Gamma(m^2))$) . The power density backscattered by this object, at its position r, is:

$$P_{refl} = P'_t \frac{G_t}{4\pi r^2}\Gamma \tag{S2}$$

Radars detect this reflected power and use different methods to estimate the distance r of its origin (for example FMCW radars use signals with frequency chirps to measure the distance to the target [Delanoë et al., 2016]). Therefore, they each measured power to a distance. We define the physical power detected from a distance r as $P'_r(r)$.

If the radar has two parallel antennas and the reflecting object is at a distance several orders of magnitude larger than the antenna separation, one can assume that the instrument is operating in full antenna overlap conditions. This means that both antennas share the same field of view at that distance. Under this assumption, we now consider the power spread caused by a wave traveling back a distance r to the radar, and the receiver antenna aperture $A_p = G_r\lambda^2/4\pi$, we get the physical power $P'_r(r)$ output at the receiver antenna end:

$$P'_r(r) = \frac{G_t P'_t}{4\pi r^2} \frac{A_p}{4\pi r^2} \Gamma = \frac{G_t G_r \lambda^2 P'_t}{(4\pi)^3 r^4} \Gamma \tag{S3}$$

Equation (S3) is known as the General Radar Equation. From this equation it is theoretically possible to retrieve the Γ value of a target from $P'_r(r)$ measurements.

Radar operators work with power variables defined by the pair $P'_t = P_t/L_t$ and $P_r(r)' = P_r(r)L_r$. Here L_t and L_r represent the total loss introduced by hardware elements, calculated as the product of all loss terms divided by all the gain terms. P_t is the power input at the emitter input and $P_r(r)$ is the power received at the receiver end, from a distance r. Usually only P_t and $P_r(r)$ are known, but the total system loss is not. This happens because it is difficult to quantify all the internal radar gains and losses. Antenna gain and radome attenuation also plays a role, increasing the amount of characterizations needed [Anagnostou et al., 2001]. This is what motivates the research of alternative calibration methods.

Another important term in the radar equation is the atmospheric attenuation $L_{at}(r)$. Attenuation is introduced by the presence of gases, which absorb power from the propagating wave. This attenuation can be significant for W band radars. For example at our site it can be reach values of $\approx 0.8\ dB\ km^{-}1$ in the horizontal, depending on absolute humidity and pressure conditions. Including atmospheric attenuation, Eq. (S3) becomes:

$$P_r(r) = \frac{G_t G_r \lambda^2 P_t}{L_r L_t (4\pi)^3} \frac{\Gamma}{L_{at}(r)^2 r^4} \tag{S4}$$

We now define the constant terms of Eq. (S4) as the RCS calibration term C_Γ (Eq. (S5)). This term enables the calculation of an observed RCS Γ from $P_r(r)$ measurements, by using the Radar Equation (Eq. (S6)). Atmospheric attenuation can be estimated from measurements of atmospheric properties and the use of microwave propagation models, such as the one proposed by Liebe [1989].

$$C_\Gamma = \frac{L_t L_r (4\pi)^3}{G_t G_r \lambda^2 P_t} \tag{S5}$$

$$\Gamma = C_\Gamma\ L_{at}^2 r^4 P_r \tag{S6}$$

As indicated previously, the calculation of C_Γ is difficult to do from an internal system characterization, due to the large amount of components and the possible interactions they may have. However, other methods exist. From Eq. (S6) it is possible to infer that by placing a discrete object with known cross section $\Gamma = \Gamma_0$ at a known distance r_0, while monitoring atmospheric conditions, allows to retrieve *externally* the calibration term C_Γ (Eq. (S7)) from sampling the power $P_r(r_0)$ reflected back. This procedure is known as end-to-end calibration because it characterizes the complete system at once.

$$C_\Gamma = \frac{\Gamma_0}{L_{at}(r_0)^2 r_0^4 P_r(r_0)} \tag{S7}$$

Obtaining C_Γ is usually enough for many radar applications, since it enables the estimation of the RCS of an object. Nevertheless, for meteorological radars the main interest is in Equivalent Reflectivity Z_e retrievals. This parameter is a measure of the reflectivity of a volume filled with small scatterers (water droplets or ice crystals). Equivalent reflectivity has the advantage that it enables the comparison between measurements of different wavelength radars.

FMCW radars have a distance resolution δr which depends on its chirp configuration. These points of differentiated resolution are called *gates*. When the instrument operates using antennas with a Gaussian beam shape of beamwidth θ (in radians), each gate has the effective sampling volume V indicated in Eq. (S8).

$$V = \frac{\pi \delta r}{2 \ln 2} \left(\frac{r\theta}{2} \right)^2 \tag{S8}$$

Assuming that target particles are spheres with a diameter D and a size distribution per unit volume of $N(D)$, that they fill the sampling volume uniformly and that most of them have a size factor in the Rayleigh Scattering regime Wallace and Hobbs [2006], the total cross section of the volume Γ_v is:

$$\Gamma_v = \frac{\pi^5 K^2}{\lambda^4} V \int_0^\infty N(D) D^6 dD \tag{S9}$$

Where $K^2 = (\epsilon_r - 1)^2/(\epsilon_r + 2)^2$ is the dielectric factor. The dielectric factor value depends on the complex relative permittivity ϵ_r of the scatterers. From Eq. (S9) arises a microphysical definition of Z_e, in $mm^6 m^{-3}$ units, as indicated in Eq. (S10).

$$Z_e = 10^{18} \int_0^\infty N(D) D^6 dD \tag{S10}$$

Replacing Eqs. (S8), (S9) and (S10) into eq. (S4), we obtain the relationship between the radar received power and Equivalent Reflectivity (Eq. (S11)).

$$Z_e = \frac{512 \ln(2) \lambda^2 L_t L_r 10^{18}}{G_t G_r \theta^2 \pi^3 K^2 P_t \delta r} L_{at}^2 r^2 P_r \tag{S11}$$

From Eq. (S11) we define the Reflectivity Calibration term C_Z. This calibration term enables the retrieval of radar equivalent reflectivity, which is in turn related to the microphysics of the hydrometeors.

$$Z = C_Z \; L_{at}^2 r^2 P_r \tag{S12}$$

As a final remark, we can use Eq. (S13) to link C_Γ with C_Z. This is the principle used in end-to-end calibration, where we first retrieving C_Γ from a point target with known RCS and then use Eq. (S13) to calculate C_Z.

$$C_Z = \frac{8 \ln(2) \lambda^4 10^{18}}{\theta^2 \pi^6 K^2 \delta r} C_\Gamma \tag{S13}$$

S2 Geometrical RCS simulator

This simulator enables the calculation of the perceived RCS for a given geometric configuration of the system. At this point it works only for trihedral reflectors. For the radar's antenna pattern it is possible to use a Gaussian model, or to input a beam shape manually. In this document we'll only show the gaussian function, since adapting the equations to consider other shapes is straightforward.

The input arguments for the RCS simulator are shown in Fig. S2 (Left). They are explained as follows:

- Radar position, referenced at the origin O: $\vec{R_O} = (x_r, 0, h_r)$
- Radar aiming angle, referenced at the origin O_r: $\vec{Y_{O_r}} = (1, \theta_r, \phi_r)$
  - θ_r: Azimuth angle of the radar's positioner. 0° is vertical aiming.
  - ϕ_r: Azimuth angle of the positioner. The line connecting the radar and the mast base corresponds to $\phi_r = 0°$.

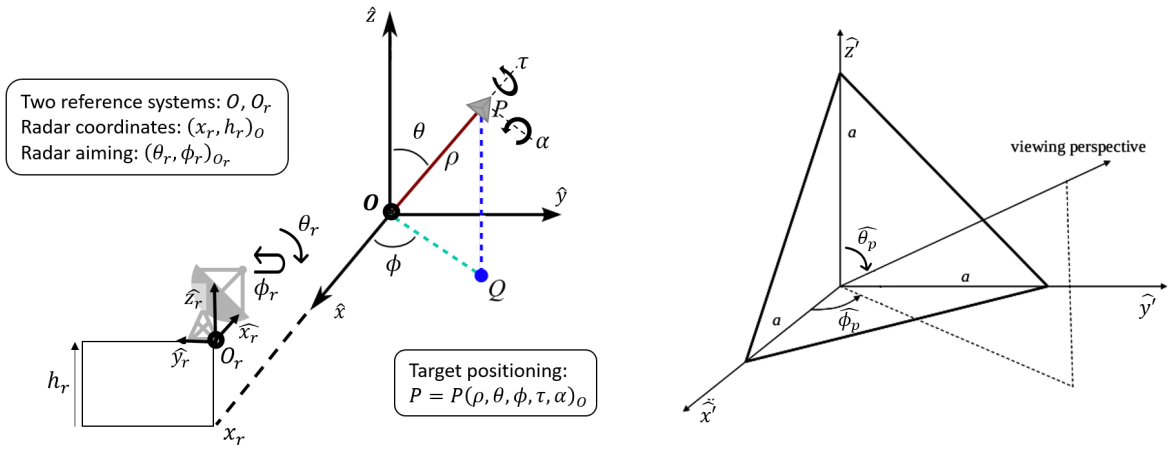

Figure S2: Diagram of the geometrical RCS simulator. (Left) shows the coordinate axes and the degrees of freedom of the simulator. (Right) shows the coordinates used to characterize the beam's incidence angle on the target. Right figure is adapted from the one published by Doerry and Brock [2009].

- Target position (in spherical coordinates), referenced at the origin O: $\vec{T_O} = (\rho, \theta, \phi)$
  - τ: Mast twist angle. $\tau = 0°$ when target boresight is parallel to the x axis.
  - α: Target tilt angle. When $\alpha = 0°$ the target's z' axis is parallel to $\hat{\rho}$. If $\alpha > 0°$ then the target tilts forward.
- a: Target's size parameter [Brooker, 2006].
- λ: Wavelength
- Antenna properties (if using Gaussian model):
  - Θ: antenna beamwidth

Output variables:

- Maximum RCS of the target $\Gamma_0[dBsm]$
- RCS of the target for the beam's incidence vector $\hat{r_i}$: $\Gamma(\vec{r_i})[dBsm]$
- Effective RCS of the target considering incidence angle and loss L due to positioning $\Delta D°$ away from the antenna's beam center: $\Gamma_{eff} = \Gamma(\vec{r_i}) - 2L(\Delta D)[dB]$

In the following sections we list the equations used to calculate each term.

S2.1 Max theoretical RCS Γ_0

From Brooker [2006], it can be simply calculated as:

$$\Gamma_0[dBsm] = 10\log_{10}(\frac{4\pi a^4}{3\lambda^2}) \tag{S14}$$

S2.2 RCS $\Gamma(\vec{r_i})$ for the beam's incidence vector

We obtain the perspective vector by changing radar aiming vector's Y_{O_r} coordinate system from O_r to O, and then multiplying by -1 to reverse the resulting vector's direction.

$$\vec{r_i} = -1\left(-(\vec{Y_{O_r}} \cdot \hat{x_r})\hat{x} - (\vec{Y_{O_r}} \cdot \hat{y_r})\hat{y} + (\vec{Y_{O_r}} \cdot \hat{z_r})\hat{z_r}\right) \tag{S15}$$

Target's unitary vectors $\hat{x'}$, $\hat{y'}$, $\hat{z'}$ (in Fig. S2 (Left)):

$$\begin{aligned}\hat{x'} = \frac{\sqrt{2}}{2}\big[-\sin(\theta)\cos(\phi)\sin(\alpha)+\cos(\theta)\cos(\phi)(\cos(\alpha)\cos(\tau)+\sin(\tau))-\sin(\phi)(\cos(\alpha)\sin(\tau)-cos(\tau))\big]\hat{x}\\ +\big[\sin(\theta)\sin(\phi)\sin(\alpha)+\cos(\theta)\sin(\phi)(\cos(\alpha)\cos(\tau)+\sin(\tau))+\cos(\phi)(\cos(\alpha)\sin(\tau)-\cos(\tau))\big]\hat{y}\\ +\big[-cos(\theta)sin(\alpha)-sin(\theta)(\cos(\alpha)\cos(\tau)+\sin(\tau))\big]\hat{z}\end{aligned} \tag{S16}$$

$$\begin{aligned}\hat{y'} = \frac{\sqrt{2}}{2}\big[-\sin(\theta)\cos(\phi)\sin(\alpha)+\cos(\theta)\cos(\phi)(\cos(\alpha)\cos(\tau)-\sin(\tau))-\sin(\phi)(\cos(\alpha)\sin(\tau)+\cos(\tau))\big]\hat{x}\\ +\big[\sin(\theta)\sin(\phi)\sin(\alpha)+\cos(\theta)\sin(\phi)(\cos(\theta)\cos(\tau)-\sin(\tau))+\cos(\phi)(\cos(\alpha)\sin(\tau)+\cos(\tau))\big]\hat{y}\\ +\big[-\cos(\theta)\sin(\alpha)-\sin(\theta)(\cos(\alpha)\cos(\tau)-\sin(\tau))\big]\hat{z}\end{aligned} \tag{S17}$$

$$\begin{aligned}\hat{z'} = \big[\sin(\theta)\cos(\phi)\cos(\alpha)+\cos(\theta)\cos(\phi)\sin(\alpha)\cos(\tau)-\sin(\phi)\sin(\alpha)\sin(\tau)\big]\hat{x}\\ +\big[\sin(\theta)\sin(\phi)\cos(\alpha)+\cos(\theta)\sin(\phi)\sin(\alpha)\cos(\tau)+\cos(\phi)\sin(\alpha)\sin(\tau)\big]\hat{y}\\ +\big[\cos(\theta)\cos(\alpha)-\sin(\theta)\sin(\alpha)\cos(\tau)\big]\hat{z}\end{aligned} \tag{S18}$$

Project perspective vector to target's coordinate system:

$$x_p = \vec{r_i} \cdot \hat{x'} \tag{S19}$$
$$y_p = \vec{r_i} \cdot \hat{y'} \tag{S20}$$
$$z_p = \vec{r_i} \cdot \hat{z'} \tag{S21}$$

Then we can calculate the perspective angles θ_p and ϕ_p:

$$p = \sqrt{x_p^2 + y_p^2 + z_p^2} \tag{S22}$$
$$\theta_p = \arccos(z_p/p) \tag{S23}$$
$$\phi_p = \arctan(y_p/x_p) \tag{S24}$$
$$\tag{S25}$$

Invalid cases: If θ_p or $\phi_p \notin [0, \frac{\pi}{2}]$, $\Gamma(\vec{r_i})$ is set to Nan (not a number). This avoids ill results that may happen in configurations where the incident beam is not impacting the interior of the reflector.

Finally, we can use valid θ_p and ϕ_p angles and the equations published by Doerry and Brock [2009] to calculate $\Gamma(\vec{r_i})$:

$$\Gamma(\vec{r_i}) = \begin{cases} \frac{4\pi}{\lambda^2} a^4 \left(\frac{4c_1c_2}{c_1+c_2+c_3} \right)^2 & \text{for } c_1 + c_2 \leq c_3 \\ \frac{4\pi}{\lambda^2} a^4 \left(c_1 + c_2 + c_3 - \frac{2}{c_1+c_2+c_3} \right)^2 & \text{for } c_1 + c_2 > c_3 \end{cases} \tag{S26}$$

For c_1, c_2 and c_3, we assign one of the terms indicated below, imposing $c_1 \leq c_2 \leq c_3$.

$$\left.\begin{matrix} c_1 \\ c_2 \\ c_3 \end{matrix}\right\} = \begin{cases} \cos(\theta_p) \\ \sin(\theta_p)\sin(\phi_p) \\ \sin(\theta_p)\cos(\phi_p) \end{cases} \tag{S27}$$

S2.3 Effective RCS Γ_{eff} considering the incidence vector and beam alignment

Since we already calculated $\Gamma(\vec{r_i})$ in the previous section, we only have left to estimate the losses $L(\Delta D)$ in the effective RCS introduced when the target is a ΔD angle away from the beam center. This calculation assumes an axially symmetric beam, but can be adjusted to consider beams with other shapes.

First, the vector connecting radar and target position:

$$\vec{\delta_O} = T_O - R_O \tag{S28}$$

We now change the origin of $\vec{\delta_O}$ from O to O_r:

$$\vec{\delta_{O_r}} = -(\vec{\delta_O} \cdot \hat{x})\hat{x_r} - (\vec{\delta_O} \cdot \hat{y})\hat{y_r} + (\vec{\delta_O} \cdot \hat{z})\hat{z_r} \tag{S29}$$

With this vector and the radar's unitary aiming vector Y_{O_r} we can proceed to calculate the angular deviation ΔD of the target from the center of the beam:

$$\Delta\theta = \arccos\left(\frac{\delta_{O_r} \cdot \hat{z_r}}{\|\delta_{O_r}\|} \right) - \theta_r \tag{S30}$$

$$\Delta\phi = \arctan\left(\frac{\delta_{O_r} \cdot \hat{y_r}}{\delta_{O_r} \cdot \hat{x_r}} \right) - \phi_r \tag{S31}$$

$$\Delta D = \sqrt{\Delta\theta^2 + \Delta\phi^2} \tag{S32}$$

$$\tag{S33}$$

And the loss, for the Gaussian antenna lobe of beamwidth Θ, is:

$$L(\Delta D) = 10\log_{10}\left(exp\left(\frac{-(2.355\Delta D)^2}{2\Theta^2} \right) \right)[dB] \tag{S34}$$

Invalid cases: We observed that for our antenna the Gaussian approximation works well if $\Delta D \leq 0.5°$ (Fig. 4 (B) of the article). Thus, we decide that any ΔD larger than $0.5°$ our calculations will return an invalid $L(\Delta D)$ value.

With all these terms and Eq. (S35) we finally calculate the effective RCS Γ_{eff}:

$$\Gamma_{eff} = \Gamma(\vec{r_i}) - 2L(\Delta D)[dB] \tag{S35}$$

S3 Misalignment bias in calibration using reference reflectors

Equation (S36) is the Radar Cross Section (RCS) calibration constant, obtained when aiming the radar towards a reference reflector of RCS Γ_0 located at a distance r_0. $L_{at}(r_0)$ represents the atmospheric attenuation between the radar and the reflector. $P_r(r_0)$ is the received power from the target position. To be correct, this equation requires a perfect alignment between the target boresight and the axis of the antenna lobe.

The RCS calibration term C_Γ can depend on additional variables, for example on temperature, due to gain changes inside the radar (Eq. (S5)). For this analysis, however, we neglect these sources of variability in the calibration and assume that $C_\Gamma = C_\Gamma^0$, with C_Γ^0 a constant defined as the calibration coefficient in the article.

$$C_\Gamma^0 = \Gamma_0 - 2L_{at}(r_0) - 40\log_{10}(r_0) - P_r(r_0) \tag{S36}$$

We define the effective RCS Γ_i as the RCS that will be observed by the radar when the target is off the beam center, or when the target is not in its designed positioning. i.e. the RCS that a perfectly calibrated radar would perceive under a non-ideal alignment.

If we use Eq. (S36) to calibrate assuming we have an RCS $= \Gamma_0$, but in reality we have an effective RCS $\Gamma_i = \Gamma_0 - \epsilon_i$, our estimated calibration term will be biased (Eq. (S37)). $C_{\Gamma i}^0$ would be the biased, experimentally retrieved calibration coefficient, C_Γ^0 the real value and ϵ_i the calibration bias.

$$C_{\Gamma i}^0 = C_\Gamma^0 + \epsilon_i \tag{S37}$$

The value of the bias term ϵ_i is difficult to estimate, because it follows an unkown distribution which depends on the alignment uncertainty of the radar, mast and target. In addition, if the average bias $\overline{\epsilon} \neq 0$ (i.e. its distribution is not zero mean), bias will not be canceled by simply averaging $C_{\Gamma i}^0$ values from multiple iterations, as indicated in Eq. (S37).

$$\frac{1}{N}\sum_{i=1}^{N} C_{\Gamma i}^0 = \frac{1}{N}\sum_{i=1}^{N}(C_\Gamma^0 + \epsilon_i) = C_\Gamma^0 + \overline{\epsilon_i} \tag{S38}$$

Figure 9 (B) of the article shows one example of a Γ_i distribution obtained from propagating uncertainty in the experiment alingment. We can clearly observe that this distribution is not zero mean. This confirms that, if no further corrections are applied, a calibration coefficient estimated by just using the average of multiple experiments is bound to have a bias $\overline{\epsilon_i}$.

To estimate the value of $\overline{\epsilon_i}$ for our setup, we use the standard deviation σ between the $C_{\Gamma i}^0$ values retrieved in each iteration as an indicator of the underlying bias distribution of the experimental setup (Eq. (S39)). It is possible to prove that this σ value is approximately equal to the standard deviation σ_ϵ of the system RCS distribution.

$$\sigma^2 = \frac{1}{N}\sum_{i=1}^{N}(C_{\Gamma i}^0 - \overline{C_{\Gamma i}^0})^2 = \sigma_\epsilon^2 \tag{S39}$$

The problem is that there are many possible uncertainty combinations in the setup that can generate distributions with the same σ_ϵ, but different expected bias $\overline{\epsilon_i}$ values. Nevertheless, by simulating a large amount of RCS distributions we can estimate the most likely bias $\overline{\epsilon_i}$, to a given degree of uncertainty. The procedure for doing this is explained in Sect. S3.1.

S3.1 Estimation of the bias term

In this section we explain how we generate a bias distribution for our setup, to estimate the bias correction term and its uncertainty. This is explained using the 20 m mast setup and the results of the 2018 campaign (Fig. 10 of the article).

We begin by simulating the distribution $f_{\overline{\epsilon_i},\sigma_\epsilon}(\overline{\epsilon_i},\sigma_\epsilon)$. This probability distribution, evaluated at the standard deviation σ observed from repeating N experiments (Eq. (S39)), provides a probability distribution for the bias.

We define this bias distribution as $\Lambda = f_{\overline{\epsilon_i}|\sigma_\epsilon}(\overline{\epsilon_i} \mid \sigma_\epsilon = \sigma)$.

To simulate $f_{\overline{\epsilon_i},\sigma_\epsilon}(\overline{\epsilon_i},\sigma_\epsilon)$ this we need to generate a large amount of $(\overline{\epsilon_i},\sigma_\epsilon)$ pairs, calculated from experiments of N iterations.

These $(\overline{\epsilon_i},\sigma_\epsilon)$ pairs are generated as follows:

1. We generate a random uncertainty set [1].
2. This uncertainty set is used to generate N random RCS values.
3. The RCS results are used to calculate a single $(\overline{\epsilon_i},\sigma_\epsilon)$ pair.
4. Repeat.

For the **20 m mast setup** we sampled the uncertainty sets used to generate the distribution $f_{\overline{\epsilon_i},\sigma_\epsilon}(\overline{\epsilon_i},\sigma_\epsilon)$ with the following functions[2]:

- $\sigma_{\theta_r} = \mathcal{U}([0°, 0.375°))$
- $\sigma_{\phi_r} = \mathcal{U}([0°, 0.375°))$
- $\sigma_\theta = \mathcal{U}([0°, 5°))$
- $\sigma_\tau = \mathcal{U}([0°, 10°))$

The region where σ_{θ_r} and σ_{ϕ_r} are sampled is within 0 and 3 times the nominal resolution of the radar positioner. For the mast angles θ and τ we have chosen to explore an space much larger than any deviation we observed during the experiments. We found that with these parameters the sampling covers a wide range of σ_ϵ values, large enough to enable a reliable estimation of the bias in our experiment.

Figure S3 shows the resulting $f_{\overline{\epsilon_i}|\sigma_\epsilon}(\overline{\epsilon_i},\sigma_\epsilon)$. We can observe that the distribution is very well defined around our results of the calibration experiment of 2018, where we got a value of $\sigma = 0.33$. It only starts to lose density only for relatively large values of $\overline{\epsilon}$ and σ_ϵ.

To avoid problems that could be introduced by the discrete nature of the simulated probability distribution, we estimate the bias distribution Λ as $\Lambda = f_{\overline{\epsilon_i}|\sigma_\epsilon}(\overline{\epsilon_i} \mid \sigma_\epsilon = \sigma \pm 5\%)$. The bias distribution obtained is shown in Fig. S4.

Since Λ is asymmetric, we use the median $\tilde{\Lambda}$ as the most likely bias for the system, and its RMSE σ_Λ as its uncertainty. This way we can now correct the bias in the calibration experiment with Eq. (S40). The total uncertainty of this estimator is indicated in Eq. (S41), with σ_i the uncertainty in the estimation of each $C^0_{\Gamma i}$ value.

$$\hat{C^0_\Gamma} = \frac{1}{N}\sum_{i=1}^{N} C^0_{\Gamma i} - \tilde{\Lambda} \tag{S40}$$

[1] The uncertainty set is the set of all uncertainties assigned to the system, for example one uncertainty set is described in Sect. 5.6 of the article.

[2] $\mathcal{U}(\cdot)$ is the continous uniform probability distribution.

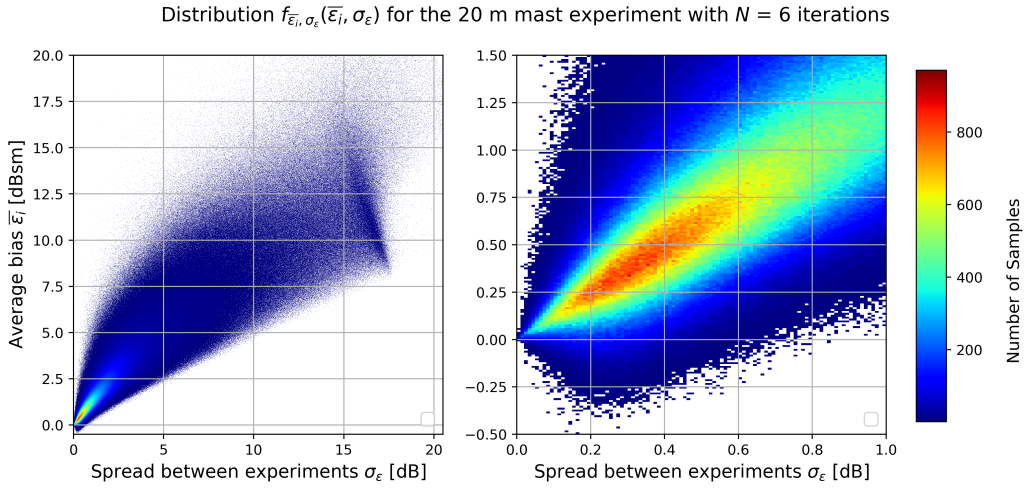

Figure S3: Simulation of $f_{\overline{\epsilon_i},\sigma_\epsilon}(\overline{\epsilon_i},\sigma_\epsilon)$. This distribution enables the estimation of the alignment bias distribution Λ by selecting the points with σ_ϵ equal to the experimentally observed σ value.

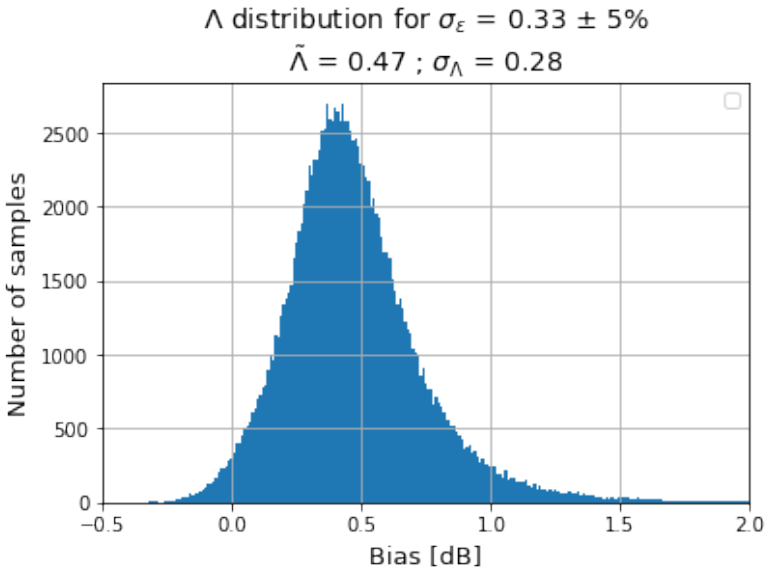

Figure S4: Estimated bias distribution Λ for the 20 m mast experiment of 2018.

$$\sigma_{\hat{C}_\Gamma^0} = \sqrt{\frac{1}{N^2}\sum_{i=1}^{N}\sigma_i^2 + \sigma_\Lambda^2} \tag{S41}$$

Finally, we include the generating functions used for the **10 m mast setup**. The use of a motor to aim the target towards the radar introduced the need of using different generating functions to sample the uncertainty sets. Apart from this the procedure remains the same as the one used for the 20 m mast.

- $\sigma_\alpha = \mathcal{U}(0, 10°)$
- $\sigma_\tau = \mathcal{U}(0, 10°))$
- $\sigma_{\theta_r} = \mathcal{U}(0, 0.375°)$
- $\sigma_{\phi_r} = \mathcal{U}(0, 0.375°)$

S4 Recommendations for future Calibration Experiments

Here we include recommendations that could be valuable for people interested in repeating the article experiment at other sites:

1. The target must be positioned far enough to avoid significant antenna overlap losses, and to avoid receiver saturation. Here a receiver saturation curve is a very valuable asset.
2. Clutter from the target environment must be properly caracterized to determine if target RCS is enough for the level of accuracy desired. Here a determination of the signal to clutter ratio becomes essential. First and second points are key to evaluate if the calibration experiment is viable.
3. Several repetitions of setup realignment and calibration sampling are necessary to estimate misalignment bias. To have a valid bias correction both radar and target must be realigned using always the same protocol. This procedure should be clearly stablished and well known by the operating team. Mast alignment in particular can be very demanding both in time and skill.
4. A characterization of radar gain variations for different internal temperatures is necessary to confirm or discard an impact in the calibration stability. This is specially important for radars built with solid state components.
5. A study on how the received power gain changes for different distances must be performed. This can be done by characterizing the IF gain in a laboratory or empirically from sampling environmental noise.
6. Atmospheric conditions must be monitored at the experiment location. We modeled attenuation at different levels based on measurements retrieved with a 20 m tower at the SIRTA observatory, and verified that a single measurement at the surface was representative for our setup. If the target is installed in a taller mast it is advisable to perform this check, to avoid biases from non-representative atmospheric attenuation modeling.
7. The experiment has to be carried out under clear conditions at the surface. No fog or precipitation is tolerable. Also wind speed should remain low ($\leq 1\ ms^{-1}$). We observed that strong wind gusts can perturb the alignment of the system, and, therefore, modify the calibration results, due to the aerodynamic resistance of the mast. We found that the best conditions for calibration at our site usually happen at nightime under clear sky conditions.
8. The use of an electronic aiming device for the target provides logistical advantages, because there is no more need of physically accesing the mast to perform re-alignments. This drastically reduced the amount of time needed to perform each iterations, from half a day with the 20 m mast setup to approximately 5 minutes with the 10 m mast.

References

J. Delanoë, A. Protat, J-P. Vinson, W. Brett, C. Caudoux, F. Bertrand, J. Parent du Chatelet, R. Hallali, L. Barthes, M. Haeffelin, et al. Basta: a 95-ghz fmcw doppler radar for cloud and fog studies. *Journal of Atmospheric and Oceanic Technology*, 33(5):1023–1038, 2016.

Emmanouil N. Anagnostou, Carlos A. Morales, and Tufa Dinku. The use of trmm precipitation radar observations in determining ground radar calibration biases. *Journal of Atmospheric and Oceanic Technology*, 18(4):616–628, 2001. doi: 10.1175/1520-0426(2001)018<0616:TUOTPR>2.0.CO;2. URL `https://doi.org/10.1175/1520-0426(2001)018<0616:TUOTPR>2.0.CO;2`.

H. J. Liebe. Mpm—an atmospheric millimeter-wave propagation model. *International Journal of Infrared and millimeter waves*, 10(6):631–650, 1989.

J. M. Wallace and P. V. Hobbs. *Atmospheric science: an introductory survey*, volume 92. Elsevier, 2006.

A. W. Doerry and B. C. Brock. Radar cross section of triangular trihedral reflector with extended bottom plate. *Sandia Report, Sandia National Laboratory*, 2009.

G. Brooker. *Sensors and signals*. Citeseer, Australian Centre for Field Robotics, Rose St Building (J04), University of Sydney, Australia, 2006.